Commun. Math. Phys. 99, 613–625 (1985)

Communications in Mathematical Physics

The Effect of Spherical Shells of Matter on the Schwarzschild Black Hole

Tevian Dray[1,2,*,**] and Gerard 't Hooft[2]

1 School of Mathematics, Institute for Advanced Study, Princeton, NJ 08540, USA
2 Instituut voor Theoretische Fysica, Princetonplein 5, Postbus 80.006, 3508 TA Utrecht, The Netherlands

Abstract. Based on previous work we show how to join two Schwarzschild solutions, possibly with different masses, along null cylinders each representing a spherical shell of infalling or outgoing massless matter. One of the Schwarzschild masses can be zero, i.e. one region can be flat. The above procedure can be repeated to produce space-times with a C^0 metric describing several different (possibly flat) Schwarzschild regions separated by shells of matter. An exhaustive treatment of the ways of combining four such regions is given; the extension to many regions is then straightforward. Cases of special interest are: (1) the scattering of two spherical gravitational "shock waves" at the horizon of a Schwarzschild black hole, and (2) a configuration involving only *one* external universe, which may be relevant to quantization problems in general relativity. In the latter example, only an infinitesimal amount of matter is sufficient to remove the "Wheeler wormhole" to another universe.

1. Introduction

In a previous paper [1], we showed the existence of a spherical gravitational shock wave at the horizon of a Schwarzschild black hole due to a massless particle located there. We show here how to generalize this result to a spherical shell of matter which joins two Schwarzschild regions, possibly of different masses. We give an exhaustive treatment of the ways of joining four Schwarzschild regions (possibly flat). We then discuss several examples of special interest, including the scattering of *two* such shells of matter, and a model for a black hole with only *one* asymptotic region.

It is particularly important to notice that by gluing Schwarzschild solutions together this way one finds solutions of the Einstein field equations with energy-momentum $T_{\mu\nu}$ corresponding to a pressureless dust cloud moving with the speed of light at the boundary. Attention is given to the physical requirement that the energy density of this matter distribution be positive. The "cloud" then consists of ordinary massless particles moving parallel to each other. It is this result that

* Supported in part by the Stichting voor Fundamenteel Onderzoek der Materie
** Permanent address: Instituut voor Theoretische Fysica, Utrecht, The Netherlands

makes our solutions highly nontrivial. It is believed that the solutions given here may be relevant to a better understanding of the quantum mechanics of black holes [2].

The paper is organized as follows. In Sect. 2 we show how to join *two* Schwarzschild regions, and in Sect. 3 we extend this to *four* Schwarzschild regions. The (straightforward) extension to *many* Schwarzschild regions, as well as several examples, are discussed in Sect. 4.

2. Two Schwarzschild Regions

It was shown in [1] that a massless particle at the horizon of a Schwarzschild black hole causes a spherical gravitational shock wave at the horizon. This is described by the metric[1],

$$ds^2 = -\frac{32m^3}{r} e^{-r/2m} du(dv + \Theta(u) df) + r^2 d\Omega^2 , \tag{1}$$

where $\Theta(u)$ is the usual step function, $f(\theta, \phi)$ represents the shift due to the shock wave, $d\Omega^2$ is the standard 2-sphere metric, and $r = r(u, v + \Theta f)$. The only nonzero component of the Ricci tensor is

$$R_{uu} = -\frac{2}{e}(\Delta f - f)\delta(u) , \tag{2}$$

where Δ is the Laplacian on S^2 and $\delta(u) = \Theta'(u)$ is the Dirac delta "function." The only nonzero component of the stress-energy tensor for a massless particle of momentum p located at the horizon ($u = 0$) at $\theta = 0$ is

$$T_{uu} = \frac{2^8 m^4 p}{e^2} \delta(\theta)\delta(u) , \tag{3}$$

where the first delta function is the (2-dimensional) delta function on the 2-sphere. The Einstein field equations can now be solved for f.

Here we instead consider a spherical shell of matter located at the horizon with stress-energy tensor given by (all other components are zero)

$$T_{uu} = \frac{\kappa}{4\pi e} \delta(u) , \tag{4}$$

where $0 \leqq \kappa = \text{constant}$, and the normalization is chosen for convenience. The Einstein field equations now yield

$$f = \kappa ; \tag{5}$$

note that the metric (1) is now C^0 *in the coordinates given.*

Summarizing the above, a spherical shell of matter at the horizon of the Schwarzschild black hole is described by the metric

$$ds^2 = -\frac{32m^3}{r} e^{-r/2m} du dv + r^2 d\Omega^2 , \tag{6a}$$

1 There exist coordinates in which this metric is C^0

where

$$-\left(\frac{r}{2m}-1\right)e^{r/2m}=\begin{cases}uv & (u\leqq 0)\\ u(v+\kappa) & (u\geqq 0)\,.\end{cases} \tag{6b}$$

The only nonzero component of the Ricci tensor is

$$R_{uu}=\frac{2\kappa}{e}\delta(u) \tag{7}$$

which, as stated before, corresponds to a cloud of massless particles moving parallel to each other if $\kappa>0$.

Technical Comment. Had we applied instead the more standard method for joining two regions, outlined in the Appendix, to the metric (6), we would obtain for the Ricci tensor not (7) but

$$R_{uu}=\frac{2\kappa}{e}\delta(u)+\frac{6\kappa^2}{e^2}\Theta(1-\Theta)\,, \tag{7'}$$

with all other components zero. We take the point of view that (7) and (7') are physically equivalent, since their difference, integrated over a test function, vanishes. In what follows we will use the convention that $\Theta(1-\Theta)=0$ in any expression containing a $\delta(u)$ term.

We now join two Schwarzschild regions of *different* (nonzero) masses, with metrics given by

$$\begin{aligned} ds^2&=-\frac{32m^3}{r}e^{-r/2m}dudv+r^2d\Omega^2\,, && (u\leqq\alpha)\,,\\ ds^2&=-\frac{32M^3}{r}e^{-r/2M}dUdV+r^2d\Omega^2\,, && (u\geqq\alpha)\,, \end{aligned} \tag{8a}$$

where $U=U(u)$, $U(\alpha)=:\beta$, $V=V(v)$, and

$$\begin{aligned} -\left(\frac{r}{2m}-1\right)e^{r/2m}&=uv\,, && (u\leqq\alpha)\,,\\ -\left(\frac{r}{2M}-1\right)e^{r/2M}&=UV\,, && (u\geqq\alpha)\,. \end{aligned} \tag{8b}$$

If $\alpha=0$, then clearly $r=2m$ at the join. But since V cannot be constant there, we also have $\beta=0$, which in turn forces $M=m$. This is just the previous case described by (6). We therefore assume $\alpha\neq 0\neq\beta$. Comparing Eqs. (8b) at $u=\alpha$ now yields

$$V'(v)=\frac{m^2\alpha}{M^2\beta}e^{-\frac{r}{2m}+\frac{r}{2M}|_{u=\alpha}}\,. \tag{9}$$

Finally, requiring that the metric (8a) be C^0 forces

$$\frac{\alpha}{m}\equiv\frac{\beta}{MU'(\alpha)}=:\gamma\,. \tag{10}$$

In the situation considered here, where there are only *two* regions, we can always choose $U=u-\alpha+\beta$. Then the metric (8) is very closely related to that of Vaidya [9], with the mass set equal to a step function. In the next section, however, we will need a more general choice of U [but we will always assume $U'(\alpha)>0$].

In general, the Vaidya metrics [9] describe space-times with a null fluid source. Hiscock [10; see also 11] constructed two-dimensional models of evaporating black holes based on [9].

Calculating the Ricci tensor as in the Appendix, the only nonzero component is

$$R_{uu}=\frac{8\delta(u-\alpha)}{\gamma r^2}(M-m), \tag{11}$$

representing a spherical shell of massless matter located at $u=\alpha$ and moving in the v-direction. Requiring that the energy density of this matter be positive forces

$$\begin{aligned}\gamma>0 &\Leftrightarrow M>m,\\ \gamma<0 &\Leftrightarrow M<m.\end{aligned} \tag{12}$$

This is depicted, together with the previously discussed case where $\gamma=0$ ($M=m$), in Fig. 1.

The above calculations for $M\neq m$ generalize a situation previously considered by Synge [3] in which one of the masses is zero, i.e. one region is flat. We thus

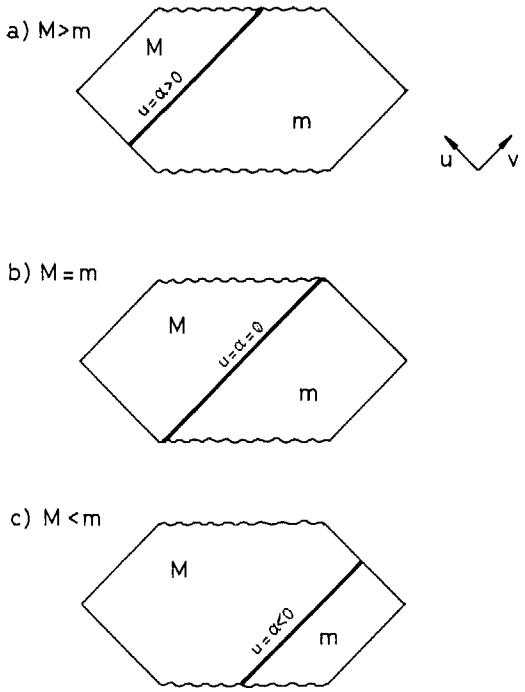

Fig. 1a–c. The location (heavy line) of the spherical shell of matter used to join two Schwarzschild regions with (positive) masses m and M, respectively. The energy density of the shell is positive. Three possibilities are shown: **a** $M>m$, **b** $M=m$, **c** $M<m$. Wavy lines represent the singularities at $r=0$; boundary lines at 45° represent null infinity

consider the case $m=0$. For convenience in the calculations of the next section we interchange the roles of u and v so that

$$\begin{aligned} ds^2 &= -4dudv + r^2 d\Omega^2, && (v \leqq a), \\ ds^2 &= -\frac{32M^3}{r} e^{-r/2M} dUdV + r^2 d\Omega^2, && (v \geqq a), \end{aligned} \tag{13a}$$

where $U=U(u)$, $V=V(v)$, $V(a)=:b$, and

$$\begin{aligned} v-u &= r, && (v \leqq a), \\ -\left(\frac{r}{2M}-1\right) e^{r/2M} &= UV, && (v \geqq a). \end{aligned} \tag{13b}$$

We can as before assume $a \neq 0 \neq b$. Comparing Eqs. (13b) at $v=a$ yields

$$U'(u) = \frac{1}{b} \frac{r}{4M^2} e^{r/2M}|_{v=a}, \tag{14}$$

and requiring that the metric be C^0 forces

$$V'(a) = \frac{b}{2M}. \tag{15}$$

We again assume $V'(a)>0$, so that $b>0$ (for positive M).

Calculating the Ricci tensor as in the Appendix, the only nonzero component is

$$R_{vv} = \frac{4M}{r^2} \delta(v-a), \tag{16}$$

representing a spherical shell of massless matter now located at $v=a$ and moving in the u-direction. Note that the total energy on any space-like hypersurface through $v=a$ is precisely the Schwarzschild mass M. This situation is shown in Fig. 2a.

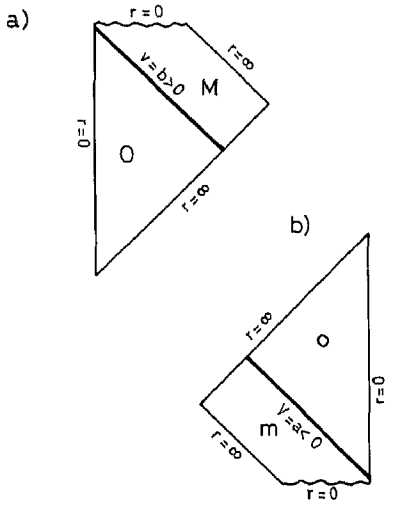

Fig. 2a and b. The global structure when a Schwarzschild region is joined to a flat region. The mass of each region is given; the spherical shell of matter used to join the two regions is indicated by the heavy line. The vertical lines labelled "$r=0$" are only *coordinate* singularities

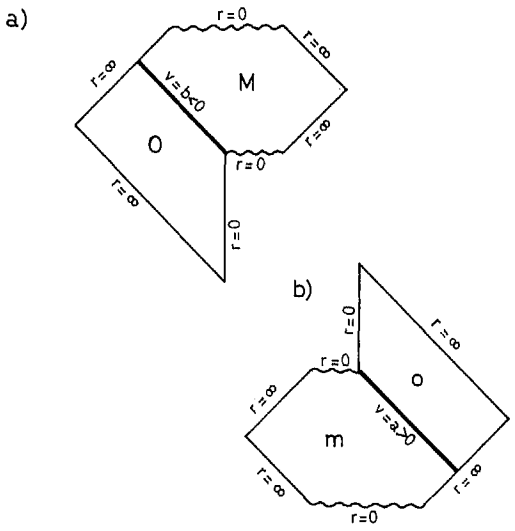

Fig. 3a and b. A different way to join a flat region to a Schwarzschild region than that depicted in Fig. 2. However, the energy density of the spherical shell of matter (heavy lines) used to join the two regions is now *negative*. The masses M and m are assumed to be positive; allowing them to be negative removes the energy density problem but changes the global structure (cf. Fig. 7)

Synge [3] considered not the above case but rather $M=0$. The mathematics is entirely analogous, except that now $r=U-V$ for $v \geqq a$, and M must be replaced by m in the Ricci tensor [Eq. 16)]. This case is shown in Fig. 2b, which is equivalent to Fig. 2 of [3], and which represents a Schwarzschild *white* hole which radiates all of its mass away.

There is another, inequivalent way to join a flat region to a Schwarzschild region. This is done by replacing the first of Eqs. (13b) by $r=u-v$. The resulting space-time is shown in Fig. 3a. However, the sign of R_{vv} is changed by this procedure, so that either the energy density at the join is negative (the case shown) or the mass M must be negative. An analogous procedure applied to Fig. 2b leads to Fig. 3b, which can be thought of as a *classical* picture of black hole evaporation. Note that the boundaries of the Penrose diagrams in Fig. 3 are no longer convex. As a rule of thumb we find that the boundary is always convex if the shells have positive energy density.

Finally, for the sake of completeness, we consider joining two flat regions. However, there are no *spherical* shells of matter in flat space analogous to the ones at the horizon of a Schwarzschild black hole discussed at the beginning of this Sect. [1]. Thus, the only way of joining two flat regions that will be considered here is given by simple identification, i.e. with no shift at all.[2]

2 However, Penrose [4] gives a different way of joining two flat regions along a spherical, *sourceless* shock wave. One could also consider *planar* shells of matter analogous to the shock waves in flat space discussed in [1]

3. Four Schwarzschild Regions

We can use the results of the last section to patch together several Schwarzschild regions. In this section we investigate the situation shown in Fig. 4, where spherical shells of massless matter at $u=\alpha$ and $v=a$ are used to join *four* Schwarzschild regions. The continuity requirements of Sect. 2 at each boundary are sufficient to yield a "reasonable" space-time. However, if no coordinates are given in which the metric is also C^0 at the point common to all four regions, then one runs the risk of having a conical singularity there. We wish to avoid such singularities, and thus require the metric to be C^0 everywhere. This will, in general, impose one constraint on the regions to be joined.

There are 17 inequivalent ways of arranging four masses in a pattern such as Fig. 4b, bearing in mind the fact that we must treat flat regions, as well as two adjacent regions with the same mass, as special cases. However, only 7 of these need to be calculated explicitly. The others are either ruled out completely by elementary considerations, reduce to a case discussed in Sect. 2, or are special cases of these 7. The 7 "fundamental" cases are shown in Fig. 5.

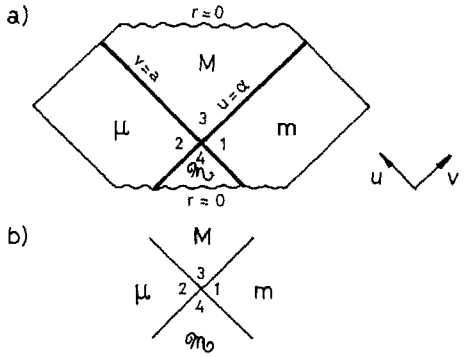

Fig. 4a and b. Four Schwarzschild regions are joined together in a C^0 manner by adding spherical shells of massless matter (heavy lines) at $u=\alpha$ and $v=\alpha$. The global structure as shown in **a** is *not* correct in general. A schematic representation of the same situation is given in **b**

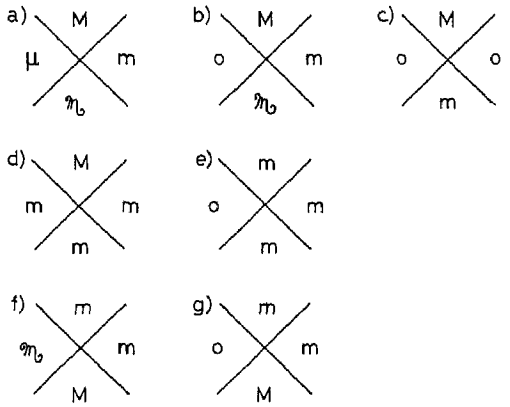

Fig. 5a–c. The seven basic ways of arranging four masses. A calculation of these seven cases enables one to calculate all possible cases

The first of these, shown schematically in Fig. 5a, is the case where all 4 masses are different and nonzero. This is described by

$$ds^2 = -\frac{32m_i^2}{r} e^{-r/2m_i} du_i dv_i + r^2 d\Omega^2 , \tag{17a}$$

$$u_i v_i = -\left(\frac{r}{2m_i} - 1\right) e^{r/2m_i}, \tag{17b}$$

where $u_i = u_i(u)$, $v_i = v_i(v)$,

$$\begin{aligned} i=1 &\Leftrightarrow u \leqq \alpha, \quad v \geqq a \\ i=2 &\Leftrightarrow u \geqq \alpha, \quad v \leqq a \\ i=3 &\Leftrightarrow u \geqq \alpha, \quad v \geqq a \\ i=4 &\Leftrightarrow u \leqq \alpha, \quad v \leqq a , \end{aligned} \tag{18}$$

as indicated in Fig. 4, and where $u = u_1$, $v = v_1$. Evaluating the continuity conditions (9) and (10) at the point $(u=\alpha, v=a)$, we obtain

$$\frac{v_j'(a)}{v_i'(a)} = \frac{m_i^2 u_i(\alpha)}{m_j^2 u_j(\alpha)} e^{r_0\left(\frac{1}{2m_j} - \frac{1}{2m_i}\right)}, \tag{19a}$$

$$m_i \frac{u_i'(\alpha)}{u_i(\alpha)} = m_j \frac{u_j'(\alpha)}{u_j(\alpha)} =: \frac{1}{\gamma_{ij}}, \tag{19b}$$

for $(i,j) = (1,3)$ or $(i,j) = (4,2)$, and

$$\frac{u_j'(\alpha)}{u_i'(\alpha)} = \frac{m_i^2 v_i(a)}{m_j^2 v_j(a)} e^{r_0\left(\frac{1}{2m_j} - \frac{1}{2m_i}\right)}, \tag{20a}$$

$$m_i \frac{v_i'(a)}{v_i(a)} = m_j \frac{v_j'(a)}{v_j(a)} =: \frac{1}{\gamma_{ij}}, \tag{20b}$$

for $(i,j) = (2,3)$ or $(i,j) = (4,1)$, where $r_0 := r(u=\alpha, v=a)$.

There are now two ways to use Eqs. (19a) and (20b) to obtain an expression for e.g. v_2', which are

$$\begin{aligned} v_2'(a) &= \frac{m_1 m_4}{m_2^2} \frac{u_4(\alpha) v_4(a)}{u_2(\alpha) v_1(a)} e^{r_0\left(\frac{1}{2m_2} - \frac{1}{2m_4}\right)} \\ &\equiv \frac{m_1^2}{m_2 m_3} \frac{u_1(\alpha) v_2(a)}{u_3(\alpha) v_3(a)} e^{r_0\left(\frac{1}{2m_3} - \frac{1}{2m_1}\right)}. \end{aligned} \tag{21}$$

Comparing the right-hand sides of these two equations and using Eqs. (17b), we finally obtain

$$(r_0 - 2m_1)(r_0 - 2m_2) \equiv (r_0 - 2m_3)(r_0 - 2m_4) . \tag{22}$$

Other combinations of Eqs. (19) and (20) yield expressions for the various $u_i'(\alpha)$ and $v_i'(a)$ but no further conditions. Equation (22) is thus the *only* additional condition [other than e.g. Eqs. (9) and (10)] which must be satisfied so that a C^0 joining of four Schwarzschild regions is possible.[3]

3 The coefficients of the delta functions in R_{uu} and R_{vv} are now automatically C^0

We will not explicitly present the analogous calculations for the cases depicted in Fig. 5b and 5c. The result is the same: Eq. (22). Furthermore, Eq. (22) is trivially satisfied for the remaining four cases shown in Fig. 5. We thus conclude that Eq. (22) must *always* be satisfied at the point where two shells of matter cross, and that it is also sufficient to guarantee the existence of a C^0 metric in a neighborhood of such a point whenever it is a nontrivial condition.

We now turn to the case shown in Fig. 5d, where three of the masses are equal and the fourth is nonzero. This situation is described by Eqs. (17) and (18), where

$$\begin{aligned} m_1 = m_4 = m_2 =: m\,, \\ m_3 =: M\,, \end{aligned} \tag{23}$$

and

$$\begin{aligned} u_1 &= u_4 + \lambda\,; \quad & v_1 &= v_4\,, \\ u_2 &= u_4\,; & v_2 &= v_4 + \kappa\,. \end{aligned} \tag{24}$$

Evaluating the continuity conditions (9) and (10) at the intersection point ($u_4 = 0, v_4 = 0$), we obtain

$$v_3'(\kappa) = \frac{m^2\lambda}{M^2 u_3(\lambda)} e^{\left(\frac{m}{M}-1\right)}, \tag{25a}$$

$$\frac{m}{\lambda} = M\frac{u_3'(\lambda)}{u_3(\lambda)} =: \frac{1}{\gamma_{13}}, \tag{25b}$$

$$u_3'(\lambda) = \frac{m^2\kappa}{M^2 v_3(\kappa)} e^{\left(\frac{m}{M}-1\right)}, \tag{26a}$$

$$\frac{m}{\kappa} = M\frac{v_3'(\kappa)}{v_3(\kappa)} =: \frac{1}{\gamma_{23}}, \tag{26b}$$

where we have used $r_0 = 2m$. Substituting e.g. Eq. (25a) into Eq. (26b) and using Eq. (17b) leads to

$$\kappa\lambda = \frac{M-m}{m} e\,. \tag{27}$$

Note that if the shifts κ and λ are positive, then $M > m$. This, then, is the additional condition which must be satisfied so that a C^0 metric describing Fig. 5d exists.[3]

The situation shown in Fig. 5e can be considered as a limiting case of Fig. 5d, and we could therefore derive the additional condition as the limit as $M \to 0$ of Eq. (27). However, because of its importance, we give the calculation explicitly. The metric in region 2 is now

$$ds^2 = -4du_2 dv_2 + r^2 d\Omega^2\,, \tag{28a}$$

with

$$v_2 - u_2 = r\,. \tag{28b}$$

Elsewhere the metric is given by Eq. (17) and (18), where

$$m_3 = m_1 = m_4 =: m\,, \tag{29}$$

and

$$\begin{aligned} u_3 &= u_1\,; \qquad v_3 = v_1 + \kappa\,, \\ u_4 &= u_1 + \lambda\,; \qquad v_4 = v_1\,. \end{aligned} \tag{30}$$

The continuity conditions (14) and (15) evaluated at the intersection point $(u=0, v=0)$ yield

$$\frac{1}{u_2'(0)} = \frac{1}{2m\kappa} e\,, \tag{31a}$$

$$\frac{1}{v_2'(0)} = \frac{\kappa}{2m}\,, \tag{31b}$$

$$\frac{1}{v_2'(0)} = \frac{1}{2m\lambda} e\,, \tag{32a}$$

$$\frac{1}{u_2'(0)} = \frac{\lambda}{2m}\,, \tag{32b}$$

where we have again used $r_0 = 2m$. Comparing, e.g. Eqs. (31a) and (32b), we obtain

$$\kappa\lambda = e\,, \tag{33}$$

which is indeed the limit as $M \to 0$ of Eq. (27)[4]

We now turn to the situation shown in Fig. 5f, where precisely two (adjacent) masses are equal and the others are nonzero. This is described by Eqs. (17) and (18), where

$$m_1 = m_3 =: m\,, \tag{34}$$

and

$$u_3 = u_1\,; \qquad v_3 = v_1 + \kappa\,. \tag{35}$$

Evaluating the continuity conditions (9) and (10) at the intersection point $(u=0, v=a)$, yields

$$u_2'(0) = \frac{m^2(a+\kappa)}{m_2^2 v_2(a)}\, e^{\left(\frac{m}{m_2} - 1\right)}, \tag{36a}$$

$$\frac{m}{a+\kappa} = m_2 \frac{v_2'(a)}{v_2(a)} =: \frac{1}{\gamma_{23}}\,, \tag{36b}$$

$$u_4'(0) = \frac{m^2 a}{m_4^2 v_4(a)}\, e^{\left(\frac{m}{m_4} - 1\right)}, \tag{37a}$$

$$\frac{m}{a} = m_4 \frac{v_4'(a)}{v_4(a)} =: \frac{1}{\gamma_{41}}\,, \tag{37b}$$

$$\frac{v_4'(a)}{v_2'(a)} = \frac{m_2^2 u_2(0)}{m_4^2 u_4(0)}\, e^{\left(\frac{m}{m_4} - \frac{m}{m_2}\right)}, \tag{38a}$$

$$m_2 \frac{u_2'(0)}{u_2(0)} = m_4 \frac{u_4'(0)}{u_4(0)} =: \frac{1}{\gamma_{42}}\,, \tag{38b}$$

4 λ has to be replaced by $-\lambda$ in going from Eq. (27) to Eq. (33) in order to compensate for the different roles of the various regions

where we have used $r_0 = 2m$. Substituting e.g. Eqs. (37b) and (38a) into Eq. (36b), and using Eqs. (17b) leads to

$$\kappa = \frac{m_4 - m_2}{m - m_4} a, \tag{39}$$

and this is the additional condition for continuity in this case.[3]

Finally, direct calculation for the case shown in Fig. 5g yields

$$\kappa = \frac{m_4}{m - m_4} a, \tag{40}$$

which is just the limit as $m_2 \to 0$ of Eq. (39), as expected.

4. Discussion

The results of the last two sections can now be used to join as many Schwarzschild regions as desired. It is only necessary that the continuity conditions of Sect. 2 be satisfied at the boundary between any two regions, and that those of Sect. 3 be satisfied at the intersection points connecting four regions.

We now discuss some of the cases shown in Fig. 5 in more detail. The situation shown in Fig. 5d describes the collision of *two* spherical shells of massless matter as described by Eqs. (6) and (7). It is remarkable that the region behind the collision (region 3) is still described by the Schwarzschild metric, but for a different mass. This is to be contrasted with the corresponding case in Minkowski space, namely the collision of two *plane* gravitational shock waves due to massless particles moving at the speed of light, which is much more difficult and for which only approximate results are available [5]. However, a quite general feature of the collision of two *sourceless* waves in flat space persists here, namely the presence of a (space-like) singularity after the collision [6].[5]

Another case of special interest is the one described by Fig. 5e and Eqs. (17), (18), and (28) thru (33). The global structure of this situation is shown in Fig. 6.

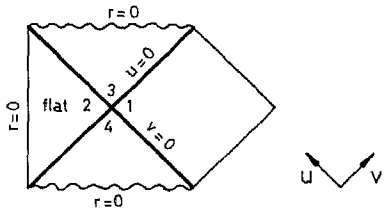

Fig. 6. The Penrose diagram for the space-time described by Fig. 5e and Eqs. (17), (18), and (28) thru (33). Region 2 now represents a *flat* region inside the black hole. The other three regions are described by the Schwarzschild metric for the same mass m. Spherical shells of massless matter (heavy lines) sit at $u=0$ and $v=0$; the metric is C^0. Note that there is only *one* asymptotic region

Note that, unlike the usual Schwarzschild metric, this space-time has only *one* asymptotic region. This could be relevant for considerations of the Hawking effect involving back-scattering [2, 7]. Note further that the energy of the ingoing (and

5 There are no *sourceless* waves in the Schwarzschild case [1]

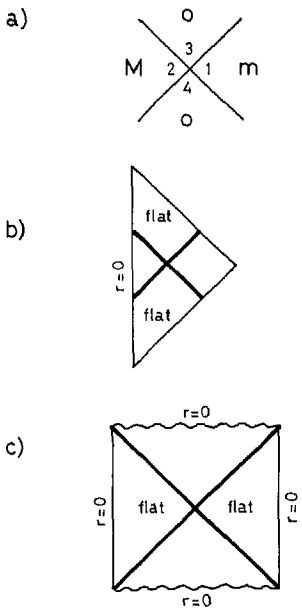

Fig. 7a–c. The scattering of two spherical shells of massless matter as described by Eqs. (13) thru (16). The mass distribution shown in **a** can only be realized if one of the masses is negative (assuming that the shells of matter, shown as heavy lines, carry positive energy density). The corresponding Penrose diagram for $M<0$ ($m>0$) is shown in **b**, while that for the mass distribution of Fig. 5c (with *positive* masses) is shown in **c**

outgoing) matter as seen by an inertial observer in the flat region 2 is just the Schwarzschild mass m, whereas a "physical" observer (at $r=$ constant in Schwarzschild coordinates) in the asymptotic region 1 sees only infinitesimal amounts of matter at $t=\pm\infty$. Since a physical black hole may have been formed by infalling matter, and may end by emission of Hawking radiation, Fig. 6 may well be a better representation of the black hole than the usual Schwarzschild metric.

Another situation which would be interesting is shown in Fig. 7a; this is just Fig. 5c with the roles of the regions interchanged. This would represent the scattering of two spherical shells of massless matter as described by Eqs. (13) thru (16) *with flat in and out regions*. However, a careful analysis of these equations (and cf. Fig. 2 and 3) shows that the *only* ways of having region 3 and/or region 4 be flat involve either a negative Schwarzschild mass or negative energy density of (one of) the shells of matter. One possibility, with positive energy density and one negative mass, is shown in Fig. 7b.[6] For comparison, in Fig. 7c we give the Penrose diagram associated with Fig. 5c; note that this space-time has *no* asymptotic region.

Appendix

Given two regions $\{u>0\}$ and $\{u<0\}$ with C^0 metrics g_{ab}, the standard [4, 8] way of joining them is to define the full metric to be

$$g_{ab}:=(1-\Theta)g^-_{ab}+\Theta g^+_{ab}, \tag{A1}$$

where $\Theta=\Theta(u)$ is the step function. Introducing the notation

$$[Q]:=\lim_{u\to 0^+} Q-\lim_{u\to 0^-} Q, \tag{A2}$$

6 No attempt has been made to keep the space-time shown in Fig. 7b C^0 at $r=0$ by requiring that both shells of matter come in from $r=\infty$ and go out to $r=\infty$

and assuming

$$[g_{ab}]=0\,, \tag{A3}$$

(so that g_{ab} is C^0) we obtain for the Christoffel symbols and Ricci tensor

$$\Gamma_{abc}=(1-\Theta)\Gamma^-_{abc}+\Theta\Gamma^+_{abc}\,, \tag{A4}$$

$$R_{ab}=(1-\Theta)R^-_{ab}+\Theta R^+_{ab}+\delta([\Gamma^u_{ab}]-[\Gamma^m_{am}]\delta^u_b) +\Theta(1-\Theta)([\Gamma^m_{ab}][\Gamma^n_{am}]-[\Gamma^m_{nm}][\Gamma^n_{ab}])\,, \tag{A5}$$

where $\delta=\delta(u)=\Theta'(u)$ is the Dirac delta "function."

Acknowledgements. We thank Roger Penrose for bringing references [3] and [9] to our attention and Lee Lindblom for showing us [10] and [11].

References

1. Dray, T., 't Hooft, G.: The gravitational shock wave of a massless particle. Nucl. Phys. B**253**, 173 (1985)
2. 't Hooft, G.: On the quantum structure of a black hole. Utrecht preprint, 1984
3. Synge, J.L.: A model in general relativity for the instantaneous transformation of a massive particle into radiation. Proc. Roy. Irish Acad. **59** A, 1 (1957)
4. Penrose, R.: In: General relativity: Papers in honour of J.L. Synge, p. 101. Ó Raifeartaigh, L. ed. Oxford: Clarendon Press 1972
5. D'Eath, P.D.: High-speed black-hole encounters and gravitational radiation. Phys. Rev. D **18**, 990 (1978); Curtis, G.E.: Twistors and linearized Einstein theory on plane-fronted impulsive wave backgrounds, and Ultrarelativistic black-hole encounters. J. Gen. Rel. Grav. **9**, 987 and 999 (1978)
6. Kahn, K.A., Penrose, R.: Scattering of two impulsive gravitational plane waves. Nature **229**, 185 (1971)
   Szekeres, P.: Colliding gravitational waves. Nature **228**, 1183 (1970)
   Szekeres, P.: Colliding plane gravitational waves. J. Math. Phys. **13**, 286 (1972)
   Nutku, Y., Halil, M.: Colliding impulsive gravitational waves. Phys. Rev. Lett. **39**, 1379 (1977)
   Chandrasekhar, S., Xanthopoulos, B.C.: On colliding waves in the Einstein-Maxwell theory. University of Chicago preprint, 1984
7. 't Hooft, G.: Ambiguity of the equivalence principle and Hawking's temperature. J. Geom. Phys. **1**, 45 (1984)
8. Taub, A.: Space-times with distribution-valued curvature tensors. J. Math. Phys. **21**, 1423 (1980)
9. Vaidya, P.C.: The gravitational field of a radiating star. Proc. Ind. Acad. Sci. A **33**, 264 (1951)
10. Hiscock, W.A.: Models of evaporating black holes. I, and -II. Effects of the outgoing created radiation. Phys. Rev. D **23**, 2813 and 2823 (1981)
11. Hiscock, W.A., Williams, L.G., Eardley, D.M.: Creation of particles by shell-focusing singularities. Phys. Rev. D **26**, 751 (1982)

Communicated by A. Jaffe

Received December 3, 1984; in revised form January 15, 1985